

Spectral and temporal dynamics of ultrashort pulses in a holmium-doped fibre amplifier

S.A. Filatova, V.A. Kamynin, I.V. Zhluktova, A.I. Trikshev, N.R. Arutyunyan, M.G. Rybin, E.D. Obratsova, D.T. Batov, V.S. Voropaev, V.B. Tsvetkov

Abstract. We have optimised a hybrid mode-locked holmium-doped fibre laser and a holmium-doped fibre amplifier for obtaining stable pulses as short as possible. Temporal and spectral characteristics of pulsed light have been measured as functions of pump power. Lasing has been achieved in the wavelength range 2066–2068 nm, with a full width at half maximum of the emission spectrum from 3 to 4 nm. The pulse duration does not exceed 1 ps and the pulse energy ranges from 0.2 to 0.5 nJ. To raise the pulse energy, holmium-doped fibre amplifiers based on two types of active fibre have been used. We have demonstrated a decrease in the width of the central part of the pulse autocorrelation function and considerable broadening of the spectrum of the pulses. The maximum average power at the amplifier output exceeds 200 mW.

Keywords: holmium-doped fibre laser, mode-locking, nonlinear polarisation rotation, hybrid mode-locking, single-walled carbon nanotubes, ultrashort pulses, holmium-doped fibre amplifier, spectral transformation.

1. Introduction

The study of the spectral and temporal dynamics of laser pulses in fibre amplifiers is a topical issue in modern optics and laser physics. Even though there is a mature method for short chirped pulse amplification [1], awarded the 2018 Nobel Prize in Physics, a search for simple, all-fibre pulse amplification systems continues to attract attention. In particular, Sidorenko et al. [2] examined picosecond pulses propagating in an ytterbium-doped fibre amplifier and taking an asymmetric temporal shape at the amplifier output. In addition, there is interest in ultrashort pulse (USP) amplifiers operating near 2 μm and at longer wavelengths, because high-energy USPs in this spectral region are much needed for dealing with

polymers and biological tissue [3, 4]. To date, a number of studies have demonstrated transformations of pulses during propagation in both thulium [4] and holmium [5, 6] fibre amplifiers. Wang et al. [5] reported considerable broadening of the pulse spectrum and narrowing of the central part of the pulse autocorrelation function (ACF) to 170 fs. It is worth noting that, in most studies concerned with transformation of pulsed light in holmium-doped fibre amplifiers, holmium-doped fibre lasers having bulk elements in their cavity were used as master oscillators (MOs). One optimal solution for obtaining an all-fibre laser system with a self-starting pulse source is to employ hybrid mode-locked MOs [7–9]. Note also that reports dealing with USP amplification do not compare transformation of pulsed light at different holmium concentrations in the active fibre of the amplifier or at different fibre lengths.

In this paper, we present experimental data on the temporal and spectral dynamics of USPs in holmium-doped fibre amplifiers. To obtain such pulses, we optimised an MO with the aim of producing a self-starting and self-reproducing light source [9].

2. Experimental setup

2.1. Master oscillator

Figure 1 shows a schematic of an all-fibre hybrid mode-locked holmium laser. The pump source used was a cw ytterbium-doped fibre laser emitting at 1125 nm, with a maximum output power of up to 8 W. The pump beam entered the ring

S.A. Filatova, V.A. Kamynin, I.V. Zhluktova, A.I. Trikshev Prokhorov General Physics Institute, Russian Academy of Sciences, ul. Vavilova 38, 119991 Moscow, Russia; e-mail: films2910@gmail.com;
N.R. Arutyunyan, M.G. Rybin, E.D. Obratsova Prokhorov General Physics Institute, Russian Academy of Sciences, ul. Vavilova 38, 119991 Moscow, Russia; Moscow Institute of Physics and Technology (State University), Institutskii per. 9, 141701 Dolgoprudnyi, Moscow region, Russia;
D.T. Batov, V.S. Voropaev Research and Academic Center 'Photonics and Infrared Technology', Bauman Moscow State Technical University, Vtoraya Baumanskaya ul. 5/1, 105005 Moscow, Russia;
V.B. Tsvetkov Prokhorov General Physics Institute, Russian Academy of Sciences, ul. Vavilova 38, 119991 Moscow, Russia; National Research Nuclear University MEPhI (Moscow Engineering Physics Institute), Kashirskoe sh. 31, 115409 Moscow, Russia

Received 17 October 2019
Kvantovaya Elektronika 49 (12) 1108–1111 (2019)
Translated by O.M. Tsarev

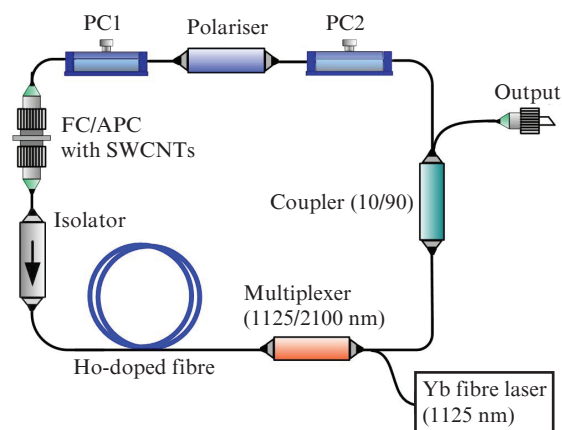


Figure 1. Schematic of the hybrid mode-locked holmium-doped fibre laser: (PC1, PC2) polarisation controllers; (SWCNTs) single-walled carbon nanotubes.

cavity of the holmium fibre laser about 10 m in length through a 1125/2100 nm fibre-optic multiplexer.

The ring cavity of the laser consisted of holmium-doped fibre (4 m long) and SMF-28e single-mode fibre (6 m long). The active fibre was produced by the MCVD process and had a core-cladding refractive index difference of 0.007, core diameter of 16 μm and cutoff wavelength of $\sim 2 \mu\text{m}$. The holmium concentration in the fibre was $5 \times 10^{19} \text{ cm}^{-3}$ and the absorption coefficient of the fibre at the pump wavelength (1125 nm) was 5 dB m^{-1} , as determined by the cut-back technique. The net cavity dispersion of the laser was evaluated using a formula proposed by Kadel and Washburn [10] and was found to be about -1.1 ps^2 .

To select one laser beam propagation direction, we used a fibre isolator operating at wavelengths above $2 \mu\text{m}$. It had a forward loss of 0.6 dB and reverse isolation greater than 30 dB. The light was outcoupled from the laser cavity using a 10/90 fibre coupler, which allowed 90% of the optical power to be outcoupled. Hybrid mode-locking was ensured by combining a fast and a slow saturable absorber in the laser cavity. The fast saturable absorber employed the nonlinear polarisation rotation effect. For this purpose, a fibre polariser and a pair of polarisation controllers were placed in the laser cavity. As a slow saturable absorber, we used single-walled carbon nanotubes (SWCNTs), which were uniformly spread on a transparent carboxymethylcellulose (CMC) film. The film and nanotubes were fixed between the ferrules of an FC/APC, which were located in the laser cavity after the isolator in order to reduce the power density.

The preparation and characteristics of suspensions of separate SWCNTs in an aqueous 1% CMC solution were described in detail elsewhere [11, 12]. Such films were previously used in erbium- and thulium-doped fibre lasers [13, 14]. Since in this study the centre emission wavelength of the holmium-doped fibre laser was shifted to longer wavelengths ($\lambda > 2050 \text{ nm}$), we used TuBall commercially available nanotubes of large diameter (more than 2 nm).

2.2. Amplifier

Ultrashort pulses from the MO were amplified by a holmium-doped fibre amplifier. Figure 2 shows a schematic of the experimental setup. The light from the MO was directed to the amplifier through a 1/99 fibre coupler, so that we were able to monitor characteristics of the MO. An isolator was used to suppress feedback at the MO output. The amplifier was pumped in a counterpropagating configuration through a multiplexer by the output of a cw ytterbium-doped fibre

laser operating at a wavelength of 1125 nm. The pump power was varied from 0 to 8 W. As the gain medium of the amplifier, we used fibres doped with holmium ions to concentrations of 6.5×10^{19} and $2 \times 10^{19} \text{ cm}^{-3}$ (fibre lengths of 2 and 4.6 m, respectively). The dispersion of the holmium-doped fibres was estimated at $-0.11 \text{ ps}^2 \text{ m}^{-1}$. At the amplifier output were placed an isolator and polarisation controller for matching with the measuring system and preventing feedback.

The laser output characteristics were assessed using the following instruments: optical spectrum analyser (Avesta, ASP-IR-2.6), 3-GHz RF spectrum analyser (Rohde & Schwartz, FSL3), ET 5000A 10-GHz photodetector, 200-MHz oscilloscope (Tektronix, TDS 2022C) and autocorrelator (APE, Pulse Check 15).

3. Results and discussion

3.1. Master oscillator

Stable pulsed lasing was observed at a pump power $P_{\text{pump}} = 3.2 \text{ W}$. The average output power P_{av} was then 4.5 mW. Figure 3a shows the emission spectrum of the laser, with a centre wavelength $\lambda_c = 2068 \text{ nm}$ and full width at half maximum $\Delta\lambda = 3 \text{ nm}$. In addition to the central peak, the spectrum has side peaks characteristic of the soliton regime of laser operation at an anomalous cavity dispersion. The pulse repetition rate ν corresponded to the cavity length and was $\sim 19.7 \text{ MHz}$, and the pulse duration τ was $\sim 1 \text{ ps}$. It is seen in the RF spectrum that the signal-to-noise ratio is 56 dB.

Raising the pump power led to energy transfer to a dispersive wave, causing an increase in the intensity of the side peaks in the optical spectrum of the laser (Fig. 3b). This was accompanied by modulation of pulses, evidenced by the presence of satellites near the main pulse repetition rate in the RF spectrum in Fig. 3b. Moreover, we observed distortion of the pulses, and their duration decreased to 0.8 ps. Further raising the pump power led to the formation of one more pulse, which had an energetically favourable position between pulses emitted at the main frequency. Eventually, this caused doubling of the pulse repetition rate, to $\sim 39.37 \text{ MHz}$ (see the RF spectrum in Fig. 3c). In addition, we observed the shape of the optical spectrum to return to its original form, corresponding to the minimum pump power, 3.2 W. This points to a decrease in the fraction of power in the dispersive wave. The increase in pulse energy with increasing pump power can be used for achieving multi-pulse lasing (harmonic mode-locking). This method has already been actively used for pulse

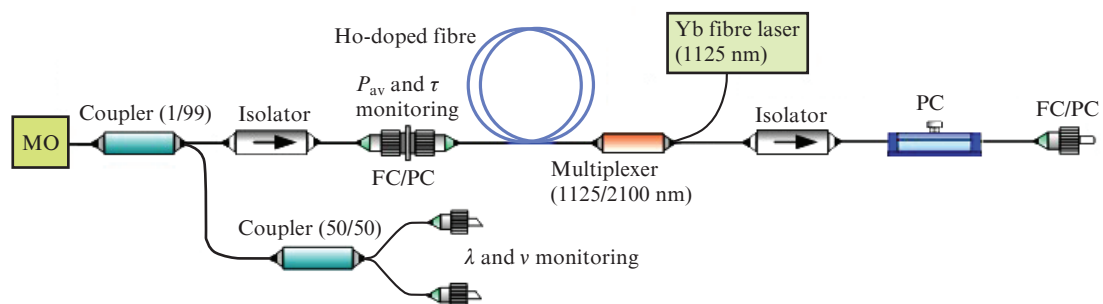


Figure 2. Schematic of the all-fibre laser system comprising an MO and holmium-doped fibre amplifier (P_{av} is the average power, τ is the pulse duration, and ν is the pulse repetition rate).

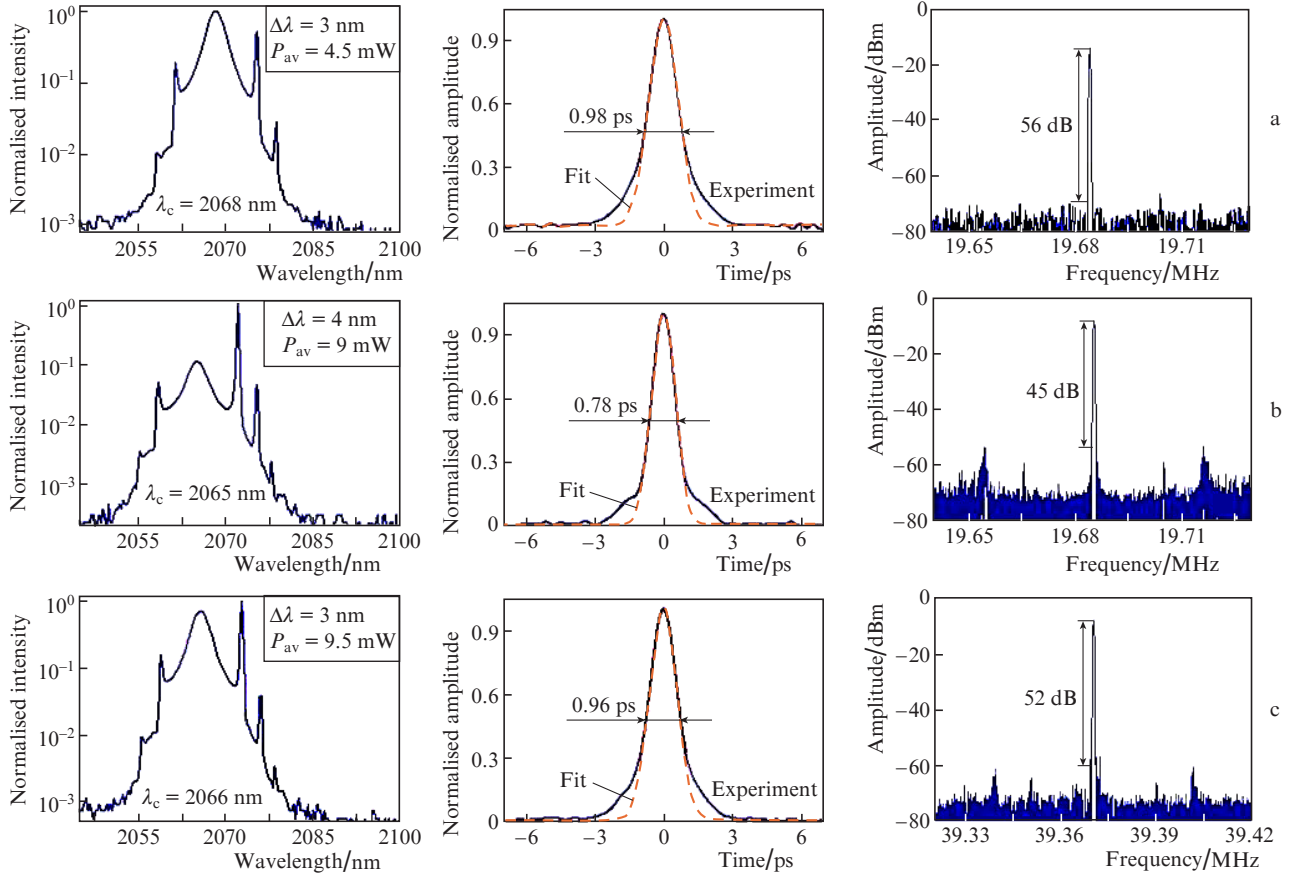


Figure 3. Laser output characteristics at pump powers of (a) 3.2, (b) 3.5 and (c) 3.6 W.

generation at a high repetition rate, for example, in erbium-doped fibre lasers [15, 16].

Table 1 compares emission characteristics of the hybrid mode-locked holmium-doped fibre laser at different pump powers.

Table 1.

P_{pump}/W	λ_c/nm	$\Delta\lambda/\text{nm}$	ν/MHz	τ/ps	P_{av}/mW	P_{peak}/W	E/nJ
3.2	2068	3	19.7	0.98	4.5	202	0.2
3.5	2065	4	19.7	0.78	9	586	0.46
3.6	2066	3	39.4	0.96	9.5	250	0.24

Thus, pump power optimisation allowed us to find a stable self-starting and self-reproducing regime necessary for further investigation of the spectral and temporal dynamics of pulses in the fibre amplifier.

3.2. Amplifier

Figures 4a and 4b show spectra and autocorrelation traces (ACTs) of light pulses at the output of a 2-m-long holmium-doped fibre amplifier with an active ion concentration of $6.5 \times 10^{19} \text{ cm}^{-3}$ at different output powers. As an input signal, we used pulses with the characteristics indicated in Table 1 for a pump power of 3.2 W.

Measurements of ACTs and spectra allowed us to follow simultaneous distortions of the spectra and pulses with increasing pump power. As seen in Fig. 4a, the pulse duration

first decreases ($P_{\text{av}} = 18$ and 82 mW), but the spectra retain a smooth shape (while the Kelly sidebands grow). Characteristically, the first-order soliton persists in this step, and the contribution of stimulated Raman scattering (SRS) is extremely small. Further raising the pump power leads to higher order soliton generation, allowing a shorter pulse duration to be obtained [5]. A further increase in pump power causes pulse decay and Raman soliton generation. The spectra take a jagged shape (Fig. 4b, $P_{\text{av}} = 160$ and 216 mW) and the ACTs contain three well-defined peaks corresponding to decaying pulses.

The use of a 4.6-m length of the fibre with the lower active ion concentration ($2 \times 10^{19} \text{ cm}^{-3}$) leads to similar spectral and temporal dynamics. It is reasonable to assume that a major contribution to pulse decay is made by the fibre of the isolator and polarisation controller.

Thus, to minimise the pulse duration in a one-stage amplifier, a balance should be maintained between the gain and the combined effect of dispersion and nonlinearity on USPs.

4. Conclusions

To optimise the holmium-doped fibre laser configuration, we have changed the location of connectors with nanotubes so as to reduce the optical power density. The length of the holmium-doped fibre has decreased to 4 m and, accordingly, the total cavity length has decreased to $\sim 10 \text{ m}$. Moreover, the pulse repetition rate has increased to $\sim 19.7 \text{ MHz}$, which corresponds to the cavity length. We have studied temporal and spectral characteristics of the laser output as functions of

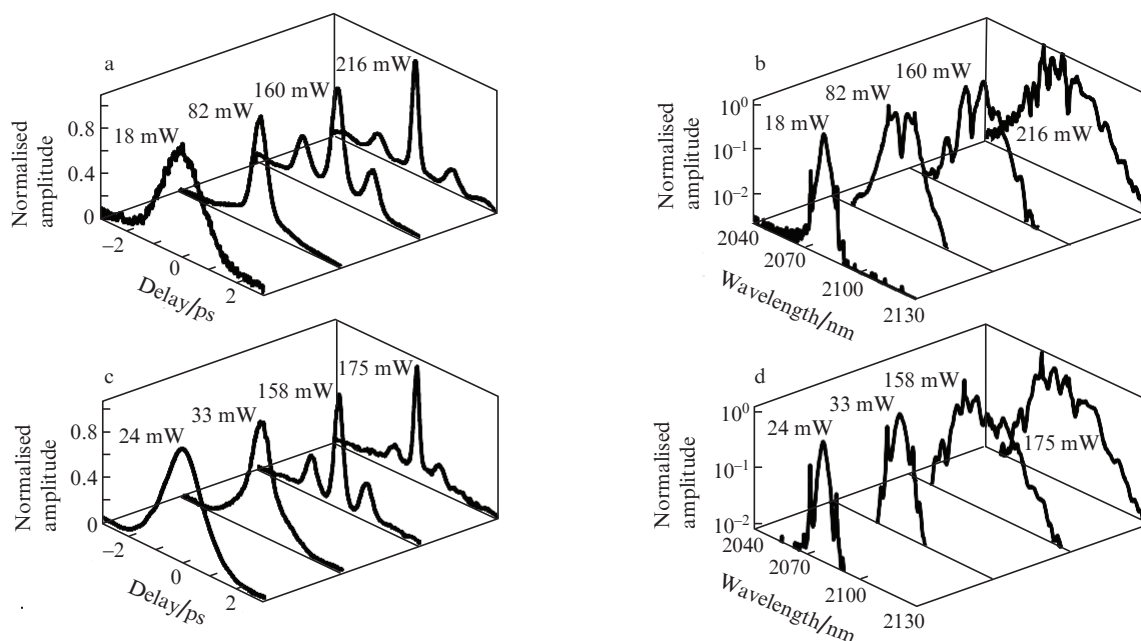


Figure 4. (a, c) ACTs and (b, d) spectra of light pulses at the output of a holmium-doped fibre amplifier with active ion concentrations of (a, b) 6.5×10^{19} and (c, d) $2 \times 10^{19} \text{ cm}^{-3}$ at different P_{av} powers.

pump power. The optimisation of the MO has made it possible to achieve stable self-starting and self-reproducing lasing with an average power of 5 mW and pulse duration of 1 ps.

In addition, we have studied the temporal and spectral dynamics of USPs propagating in holmium-doped fibre amplifiers with active ion concentrations of 2×10^{19} and $6.5 \times 10^{19} \text{ cm}^{-3}$. The width of the central part of the pulse ACF has been shown to decrease, along with considerable broadening of the spectrum of the pulses. We have obtained pulsed radiation with more than 200 mW of average power at wavelengths above 2 μm .

Acknowledgements. This work was supported by the Russian Foundation for Basic Research (Research Project No. 19-32-90205).

References

1. Strickland D., Mourou G. *Opt. Commun.*, **55** (6), 447 (1985).
2. Sidorenko P., Fu W., Wise F.W. *Proc. Eur. Conf. on Lasers and Electro-Optics* (Munich, 2019) C. cj_7_6.
3. Scholle K., Lamrini S., Koopmann P., Fuhrberg P. *Frontiers in Guided Wave Optics and Optoelectronics* (London: Intech Open, 2010) p. 471.
4. Elahi P., Kalaycioglu H., Akcaalan O., Cagri Senel C., Ilday F.O. *Opt. Lett.*, **42** (19), 3808 (2017).
5. Wang M., Zhang H., Wei R., et al. *Opt. Lett.*, **43** (19), 4619 (2018).
6. Hinkelmann M., Wandt D., Morgner U., Neumann J., Kracht D. *Opt. Express*, **25** (17), 20522 (2017).
7. Dvoretiskii D.A., Sazonkin S.G., Voropaev V.S., Negin M.A., Leonov S.O., Pnev A.V., Karasik V.E., Denisov L.K., Krylov A.A., Davydov V.A., Obraztsova E.D. *Quantum Electron.*, **46** (11), 979 (2016) [*Kvantovaya Elektron.*, **46** (11), 979 (2016)].
8. Chernysheva M., Bednyakova A., Al Araiimi M., Howe R.C., Hu G., Hasan T., Gambetta A., Galzerano G., et al. *Sci. Rep.*, **7**, 44314 (2017).
9. Filatova S.A., Kamynin V.A., Arutyunyan N.R., Pozharov A.S., Trikshev A.I., Zhluktova I.V., Zolotovskii I.O., Obraztsova E.D., Tsvetkov V.B. *J. Opt. Soc. Am. B*, **35** (12), 3122 (2018).
10. Kadel R., Washburn B.R. *Appl. Opt.*, **51** (27), 6465 (2012).
11. Krylov A.A., Sazonkin S.G., Arutyunyan N.R., Grebenyukov V.V., Pozharov A.S., Dvoretiskiy D.A., Obraztsova E.D., Dianov E.M. *J. Opt. Soc. Am. B*, **33** (2), 134 (2016).
12. Chernysheva M.A., Krylov A.A., Arutyunyan N.R., Pozharov A.S., Obraztsova E.D., Dianov E.M. *IEEE J. Sel. Top. Quantum Electron.*, **20** (5), 448 (2014).
13. Tausenev A.V., Obraztsova E.D., Lobach A.S., Chernov A.I., Konov V.I., Kryukov P.G., Konyashchenko A.V., Dianov E.M. *Appl. Phys. Lett.*, **92** (17), 171113 (2008).
14. Solodyankin M.A., Obraztsova E.D., Lobach A.S., Chernov A.I., Tausenev A.V., Konov V.I., Dianov E.M. *Opt. Lett.*, **33** (12), 1336 (2008).
15. Trikshev A.I., Kamynin V.A., Tsvetkov V.B., Itrin P.A. *Quantum Electron.*, **48** (12), 1109 (2018) [*Kvantovaya Elektron.*, **48** (12), 1109 (2018)].
16. Chen H., Chen S.P., Jiang Z.F., Hou J. *Opt. Express*, **23** (2), 1308 (2015).